A Diagrammatic Study of Gauge and Gravity Amplitude Relations

Bachelor Thesis in Physics, 15 c

Micah Tegevi

Supervisor: Gregor Kälin
Subject reader: Marco Chiodaroli

Department of Physics and Astronomy
Division of Theoretical Physics
Uppsala University
June 22, 2018

ABSTRACT

We review modern methods of scattering amplitude computations, beginning with color-decomposition that decomposes the amplitude into a color-dependent and a color-independent part of partial color-ordered amplitudes. We then show how a full amplitude can be described through the color-factor, propagator structure, and kinematic numerator of cubic color-ordered diagrams. The color-factors obey a Lie algebra and as such satisfy the Jacobi identity. We are able to impose the color-kinematics duality that states that the kinematic numerators also obey this identity. Because of this it is possible to write down sets of Jacobi equations for the numerator through their diagrammatic expression. These can be solved for a set of master numerators through which all other numerators can be expressed linearly. We find such solutions for the tree-level, one-loop, and two-loop diagrams for any number of particles.

SAMMANFATTNING

Vi ger en genomgång av moderna metoder som används vid beräkningar av spridningsamplituder. Först beskriver vi färg-dekomposition (eng: color-decomposition) där amplituden delas upp i en färgberoende del och en färgoberoende del bestående av partiella färgdordnade amplituder. Därefter visar vi hur en fullständig amplitud kan beskrivas genom färgfaktorn, propageringsstrukturen, samt den kinematiska täljaren för kubiska färgordnade diagram. Då färgfaktorerna följer en liealgebra så uppfyller de Jacobi identiteten. Vi kan införa den färg-kinematiska dualiteten som säger att även de kinematiska täljarna uppfyller denna identitet. Som en följd av detta är det möjligt att skriva ned ekvationssytem bestående av Jacobi ekvationer för täljarna genom deras diagrammatiska representation. Ekvationssystemen kan lösas för ett set av så kallade master täljare genom vilka alla andra täljare kan beskrivas linjärt. Vi hittar sådana lösningar för diagrammen på träd, en loop, samt två loop nivåerna som håller oavsett antalet partiklar.

CONTENTS

1 INTRODUCTION

Scattering amplitudes are a measure of the probability for a particle scattering event to occur. This probability can be meassured experimentally by detectors at high-energy experiments such as the LHC. To be able to compare experiment with theory the accuracy of the theoretical predictions must match the precision of the experiments. As technology advances and measuremnts become more precise the need to include higher orders of perturbation in the theoretical calculations is imporant to improve their accuracy. A common method for calculating scattering amplitudes is using Feynman diagrams and their accompanying mathematical rules which depend on the theory used [1]. Each possible Feynman diagram contributes to the total amplitude which is calculated summing over all contributions. It is a very straightforward method that in theory always works but is only applicable at low perturbation orders and for events with few particles. As the particles and order of perturbation increases the number of diagrams increases rapidly. For example the growth is factorial with respect to the number of particles n, for tree-level the number of diagrams increase like $((n-3)!)^2$ [2]. With such an increase in diagrams the mathematical expressions become very large and computationally demanding for modern computers. Moreover the resulting expressions are usually quite simple in comparison. The reason being that there are a lot of redundant terms in the expressions, arising from the fact that the total amplitude is gauge invariant whereas the individual contributions are not.

Another problem in physics is the unification of the fundamental interactions into a single theory. All forces except gravity can be described well through gauge theories in the framework of quantum field theories such as quantumchromodynamics which describes the strong interaction. Gravity, however, has proven troublesome to reconcile with quantum theories. Furthermore gravity amplitude calculations are even more demanding than gauge amplitude calculations. This is because most gravity theories are non-renormalizable and the Feynman rules for gravity are more complicated than for gauge theories.

Newer and better methods are needed and work in the recent years has proven fruitful. These use various recursion techniques and relations between diagrams to calculate scattering amplitudes more efficiently. As the contributions are not all independent it is possible to find a basis of partial color-ordered amplitudes that can be used to express the full amplitude. A relation was found by Bern, Carrasco, and Johansson that reduces the number of independent color-ordered tree-level amplitudes $(n-3)!$ [2]. This arises from a duality called the color-kinematics duality that when imposed also reveals a double-copy relation between gauge theory and gravity.

In this thesis we will give an overview of relations between color-ordered amplitudes, their corresponding diagrammatic identities, and the connection between gauge and gravity theories. The focus will be on the kinematic factors and their corresponding diagrammatic representation. We will study the topology of different sets of diagrams and see how basis sets of independent diagrams can be constructed from these.

In section 2 we will give an overview of relations between color-ordered amplitudes and a summary of how they are achieved. We will also talk about the connection found between gauge- and gravity theories.

Section 3 shows how color-ordered amplitudes can be described through diagrams and how these diagrammatic identities follow the relations from section 2. This will lead to the ability of writing down sets Jacobi equations for the amplitudes in a diagrammatic representation.

Section 4 we describe the code written to generate equations and present general solutions for the Jacobi equations for tree-level, one-loop, and two-loops.

We end with section 5 where we discuss the contents of the report and talk about possibilities of extending the work.

2 REVIEW

2.1 Feynman rules and color decomposition

To fully understand the power of modern techniques for calculating scattering amplitudes it is useful to have an insight into how scattering amplitudes are calculated using Feynman rules.

The language of gauge field theories is used to describe all fundamental forces except gravity and work is being done reconciling gravity with gauge theories. As mentioned the classical method of calculating scattering amplitudes is writing down the mathematical expression for each diagram and adding it all together. Each gauge theory comes with its own sets of Feynman rules. However there is a choice in how to pick the rules, this is called choosing a gauge, and generally means that the individual contributions from each diagram are not gauge invariant. In accordance with the symmetry of the theories the resulting scattering amplitude is gauge invariant.

With the common Feynman gauge for Yang-Mills the Feynman rules for a propagating gluon, a three-gluon vertex, and a four-gluon vertex are [1]

$$= \frac{-i\eta_{\mu\nu}\delta^{ab}}{q^2}, \tag{1a}$$

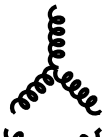

$$= -g_s f^{abc}(\eta^{\mu\nu}(p-q)^{\lambda} + \eta^{\nu\lambda}(q-r)^{\mu} + \eta^{\lambda\mu}(r-p)^{\nu}), \tag{1b}$$

$$\begin{aligned} &= -ig_s^2(f^{eac}f^{ebd}(\eta^{\mu\nu}\eta^{\lambda\rho} - \eta^{\mu\rho}\eta^{\nu\lambda}) + f^{ead}f^{ebc}(\eta^{\mu\nu}\eta^{\lambda\rho} - \eta^{\mu\lambda}\eta^{\nu\rho}) \\ &\quad + f^{eab}f^{ecd}(\eta^{\mu\lambda}\eta^{\nu\rho} - \eta^{\mu\rho}\eta^{\nu\lambda})). \end{aligned} \tag{1c}$$

In these the indices (a,b,c,d) are the colour indices for each external vertex and (μ,ν,λ,ρ) the Lorentz indices for the vertices. The 4-momenta are denoted q,p, and r. δ^{ab} is the Kronecker delta, and the Minkowski metric is

$$\eta = \text{diag}(1, -1, -1, -1). \tag{2}$$

The variable g_s is a coupling constant associated with the strong force. Gauge theories contain Lie-algebra valued fields in which the color factors f^{abc} are structure constants. They are related to the generators of the Lie algebra

$$f^{abc}T^c = [T^a, T^b]. \tag{3}$$

It is common to normalise eq. (3) by putting a coefficient on the left hand side, for example i, but this is not a necessity.

Two properties of a Lie algebra are that the generators are antisymmetric

$$[T^a, T^b] = -[T^b, T^a], \tag{4}$$

and that they satisfy the Jacobi identity

$$[T^a, [T^b, T^c]] + [T^b, [T^c, T^a]] + [T^c, [T^a, T^b]] = 0. \tag{5}$$

As the structure constants are related to the generators it can be shown that they too satisfy anticommutativity

$$f^{abc} = f^{bca} = f^{cab} = -f^{acb} = -f^{cba} = -f^{bac}, \tag{6}$$

and the Jacobi identity

$$f^{abe}f^{ecd} + f^{ace}f^{edb} + f^{ade}f^{ebc} = 0. \tag{7}$$

Looking at eqs. (1a) to (1c) we understand how these expressions become unmanageable as the number of diagrams increases. For loop diagrams there is also an integral over the loop momenta for each loop to take into account. There exist similar rules for graviton-graviton interactions and these are even more extensive.

There are a number of tools and relations useful to reduce the number of diagrams and increase the efficiency of scattering amplitude calculations. The first being color-decomposition [3, 4] where the main idea is that the amplitude is decomposed into two parts, one containing partial amplitudes which include the kinematic information, and one containing color-algebra information. The color information can be written as a trace over the generators. Thus the total color-dressed tree-level amplitude can be expressed as

$$\mathcal{A}_n^{tree}(1, 2, \ldots, n) = \sum_{\sigma \in \mathrm{perm}(2,\ldots,n)} \mathrm{Tr}(T^{a_1}T^{a_{\sigma(2)}} \cdots T^{a_{\sigma(m)}}) A_m^{tree}(1, \sigma), \tag{8}$$

with σ being the permutations of the labels 2,3,$\ldots$, n. A_m are called partial amplitudes or color-ordered (tree-level) amplitudes. They can be computed using color-ordered Feynman rules [4].

Decomposing the diagrams in such a way is useful as there are relations between the color-ordered amplitudes. There is cyclic symmetry [4]

$$A_m^{tree}(1,2,\ldots,n) = A_m^{tree}(2,\ldots,n,1), \tag{9}$$

reflection antisymmetry [4]

$$A_m^{tree}(1,2,3,\ldots,m-1,m) = (-1)^m A_m^{tree}(1,m,m-1,\ldots,3,2), \tag{10}$$

and photon decoupling

$$\sum_{\sigma \in cyclicperm(2,\ldots,m)} A_m^{tree}(1,\sigma) = 0. \tag{11}$$

Relations like these decrease the number of amplitudes that contribute to the full colour-dressed amplitude. As we shall see there are still ways to continue this reduction.

2.2 Color-kinematics duality

In the above section we saw how the number of amplitudes contributing to a full amplitude can be reduced to color-ordered amplitudes. We will now reduce this even more by showing that the amplitudes can be expressed solely through cubic diagrams.

Before we begin it should be noted that the diagrams used in this paper from here on are similar to Feynman diagrams in appearance and that both types of diagrams describe particle interactions but they are not the same. These diagrams will be used to describe interactions consisting of one type of particle which can be assumed to be a force carrier, e.g. a gluon, in gauge theories or a graviton for gravity theories. As the relations we are working with are valid for both theories any such particle is a valid interpretation. Arrows in the diagrams (when drawn) describe the flow of momenta and all external particles are chosen to have outgoing momenta.

Any internal line in a diagram is called a propagator and will have an associated propagator structure which is the momenta squared. We write the propagator structure of a diagram as $d(g)$. To show that any such structure can be written in terms of cubic graphs we look at the two diagrams in fig. 1. The first diagram we call a and it has propagators with momenta p and q. Its propagator structure is

$$d(g_a) = p^2 q^2. \tag{12}$$

The second diagram is the same as a but with one of the edges contracted. Its propagator structure is

$$d(g_b) = p^2. \tag{13}$$

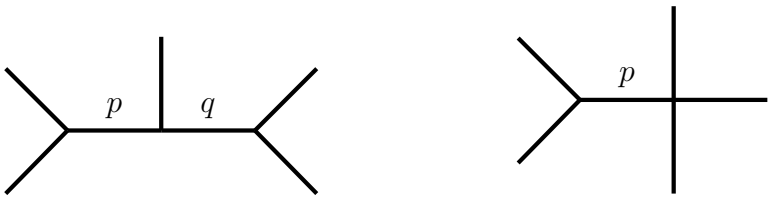

Figure 1: Two diagrams where (b) can be considered (a) but with the internal edge denoted q contracted.

We can also write this in terms of $d(g_a)$

$$d(g_b) = \frac{d(g_a)}{q^2}. \tag{14}$$

This procedure can of course be carried out for any number of edge contractions.

The color-factors are by definition already expressed in terms of cubic graphs. As an example the color-factor for the cubic vertex in eq. (1c) is simply the sum of color-factors belonging to the diagrams that are the possible ways of expanding it into a cubic diagram. The amplitude for the four-point vertex can thus be written

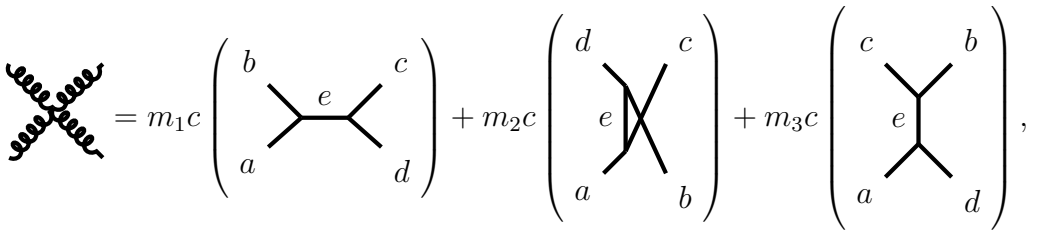

(15)

with the c denoting the color-factor for each respective diagram (e.g. $f^{abe}f^{ecd}$ for the first diagram on the RHS) and m_i containing all additional information.

Now we can rewrite eq. (8) such that it is expressed through cubic diagrams

$$\mathcal{A}_n^{tree} = \sum_{g \in \Gamma^{tree}_{n,\mathrm{UO}}} \frac{c(g)n(g)}{d(g)}. \tag{16}$$

Here the sum runs over the color-ordered tree level diagrams g with n external legs (in/outgoing particles) in the unordered set $\Gamma_{n,\mathrm{UO}^{tree}}$ containing all such diagrams. In the denominator there is the propagator structure $d(g)$, the $c(g)$ term in the nominator is the color-weight. Lastly in the nominator is the kinematic factor $n(g)$ that contains all information not included in $c(g)$ or $d(g)$.

We have already seen in section 2.1 that the color weights for the interactions are anti-

symmetric and satisfy the Jacobi identity and as such this is true also for the color-factors

$$c(g_i) = c(g_j) + c(g_k), \tag{17a}$$
$$c(g) = -c(\bar{g}). \tag{17b}$$

According to the color-kinematics duality there exists a representation where these relations are true also for the kinematic numerators. This is proven for pure gluon and quark-gluon theories at tree-level [2, 5] and conjectured to hold for all loop orders [6]. Thus we can write

$$c(g_i) = c(g_j) + c(g_k) \Leftrightarrow n(g_i) = n(g_j) + n(g_k), \tag{18a}$$
$$c(g) = -c(\bar{g}) \Leftrightarrow n(g) = -n(\bar{g}). \tag{18b}$$

Once this duality is imposed it is possible to reduce the number of partial amplitudes even more as many of them are related through antisymmetry and Jacobi relations.

Kleiss-Kuijf (KK) relations state that there exists an $(n-2)!$ dimensional basis through which every n-point colour-ordered amplitude can be linearly expressed. This was achieved by fixing the position of two of the external legs and limiting the coefficients to -1,0, and +1 [7]. The relation was later proven using the Jacobi relations between the colour factors and the antisymmetry of the kinematic numerators [8].

Lastly there are Bern-Carrasco-Johansson (BCJ) relations which reduce the basis to one of $(n-3)!$ colour-ordered amplitudes. These fix three external legs and give the coefficients as functions of Lorentz invariants. They arise form the Jacobi relations between kinematic numerators. The relations are proven to hold for all tree-level cases and conjectured to hold for all loop-levels [2, 9–12].

2.3 Double copy

Once imposed the color-kinematics duality implies a double copy between gauge and gravity theory. With kinematic numerators satisfying the duality n-point tree-level gravity amplitudes are calculated [6]

$$\mathcal{M}_n^{tree} = \sum_{g \in \Gamma_{n,\mathrm{UO}}^{tree}} \frac{n(g)^2}{d(g)}, \tag{19}$$

which is eq. (16) but with one of the color-factors $c(g)$ replaced by a corresponding kinematic numerator $n(g)$. Essentially

$$(\text{gravity}) = (\text{gauge theory})^2. \tag{20}$$

Moreover the formula can also be made valid for two different representations of the same amplitude

$$\mathcal{M}_n^{tree} = \sum_{g \in \Gamma_{n,\mathrm{UO}}^{tree}} \frac{n(g)\tilde{n}(g)}{d(g)}, \tag{21}$$

with $n(g)$ and $\tilde{n}(g)$ being the kinematic numerators corresponding to the different representations. In fact it is only needed that one of the numerators satisfy the color-kinematics duality. To show this we let $\tilde{n}(g)$ be a generalized gauge transformation of $n(g)$ defined as

$$\tilde{n} \equiv n \to n + \Delta(g). \tag{22}$$

Because of the algebraic relations of $c(g)$ it is given that

$$\sum_{g \in \Gamma_{n,\mathrm{UO}}^{tree}} \frac{c(g)\Delta(g)}{d(g)} = 0. \tag{23}$$

For eq. (16) to hold we must have

$$\sum_{g \in \Gamma_{n,\mathrm{UO}}^{tree}} \frac{n(g)\Delta(g)}{d(g)} = 0, \tag{24}$$

which proves that eq. (19) and eq. (21) are equivalent. This is a useful property when constructing supergravity theories [13], however this is not something this thesis will touch on.

This duality is proven for tree-level and conjectured to hold for all loop orders. For loop-level the gauge amplitude is [6]

$$\frac{(-i)^L}{g^{n-2+2L}} \mathcal{A}_n^{loop} = \sum_g \int \prod_{l=1}^{L} \frac{\mathrm{d}^D p_l}{(2\pi)^D} \frac{1}{S(g)} \frac{n(g)c(g)}{d(g)}, \tag{25}$$

where the sum runs over all cubic n-point L-loop diagrams. The p_l in the integration is simply the propagators in the term $d(g)$ and $S(g)$ is the internal symmetry factor related to each graph. It should be noted that the g on the LHS is the coupling constant whereas the g that the color-factor, kinetic numerator, and propagator factor are functions of are the diagrams.

For the gravity amplitude the coupling constant is exchanged for the gravitational analogue κ and the loop-level amplitude can be expressed

$$\frac{(-i)^{L+1}}{(\frac{\kappa}{2})^{n-2+2L}} \mathcal{M}_n^{loop} = \sum_g \int \prod_{l=1}^{L} \frac{\mathrm{d}^D p_l}{(2\pi)^D} \frac{1}{S(g)} \frac{n(g)\tilde{n}(g)}{d(g)}. \tag{26}$$

The existence of the double copy is both remarkable and useful as the Feynman rules for gravity theories are vastly more complicated than those for gauge theories. To be able to calculate gravity amplitudes using gauge theory amplitudes is bound to increase the efficiency of gravity computations.

3 DIAGRAM RELATIONS FOR NUMERATOR FACTORS

We now want to study the consequences of eq. (18a) in a diagrammatic way. This will be done by seeing how we can relate color-ordered diagrams through Jacobi relations.

3.1 Master topologies

Based on the relations and identities reviewed above we will study diagrammatic relations between the kinematic numerators. We work with the notion that all graphs can be reduced to cubic graphs and that the color-kinematics duality holds and therefore also BCJ-relations and the double copy.

Three diagrams which will be important are the so called Mandelstam diagrams shown in fig. 2.

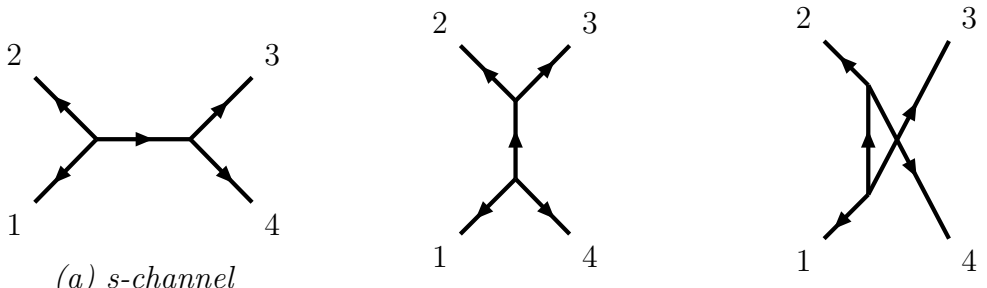

(a) s-channel *(b) t-channel* *(c) u-channel*

Figure 2: The Mandelstam diagrams.

These are called the s-channel, t-channel, and u-channel respectively and are called so because of the Mandelstam invariants. These are kinematic invariants and for massless momenta k_i defined as outgoing they are

$$s \equiv (k_1 + k_2)^2 = (k_3 + k_4)^2, \tag{27}$$
$$t \equiv (k_1 + k_4)^2 = (k_2 + k_3)^2, \tag{28}$$
$$u \equiv (k_1 + k_3)^2 = (k_2 + k_4)^2. \tag{29}$$

We define the operators $\hat{t}$ and $\hat{u}$ as the operators that take the s-channel graph and transforms it into the t- and u-channel respectively. It operates on the internal edge of the s-channel diagram and rearranges the way the edges meet at the vertices. These diagrams and operators will be our building blocks as we construct more diagrams but first we will go through how the antisymmetry and Jacobi relations look from a diagrammatic point of view.

The kinematic numerators and colour factors follow the antisymmetry identity in that when an odd number of legs are flipped they gain a minus sign but stay the same otherwise. An even number of flips returns the same color- and kinematic factors. For example exchanging legs 3 and 4 while keeping legs 1 and 2 constant will give a color factor with a sign change, flipping legs 1 and 2 also will give the same color factor. i.e

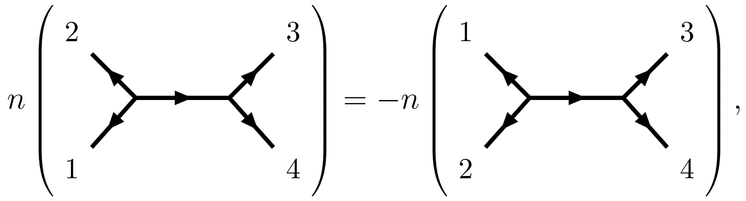

(30)

and

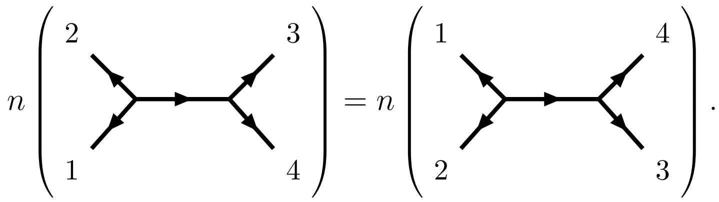

(31)

The Jacobi relations hold between the Mandelstam graphs

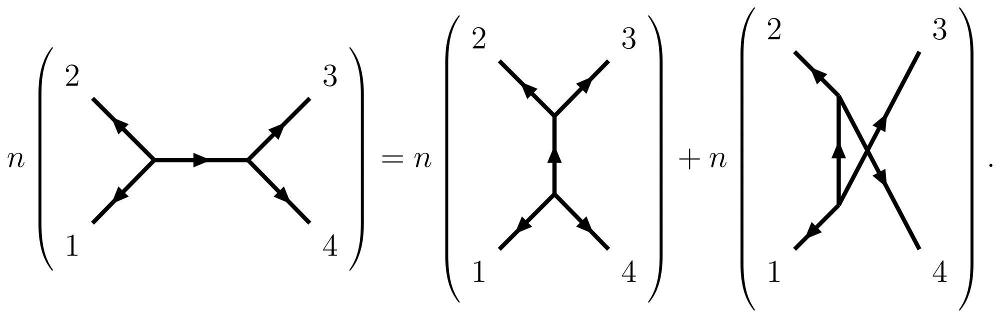

(32)

These relations of course hold for the colour factors as they satisfy the Jacobi identity.

Graphs are uniquely defined by their topology and momentum assignment. The three Mandelstam diagrams all have the same topology but different momentum assignment. The kinematic numerators depend on both of these but henceforth we will care mostly about distinct topologies.

At four-point tree-level there is only one topology for the cubic graphs. The same is true for five point as the only possible topology looks like the one at four point but with an extra external leg on the internal leg. At six-point tree-level there are two topologies as shown in fig. 3.

If we apply one of the operators $\hat{t}$ or $\hat{u}$ to one of the internal edges in the branched graph (b) it will be transformed into the half-ladder graph (a). Hence there exists a Jacobi relation between the corresponding numerators and they can be expressed through each

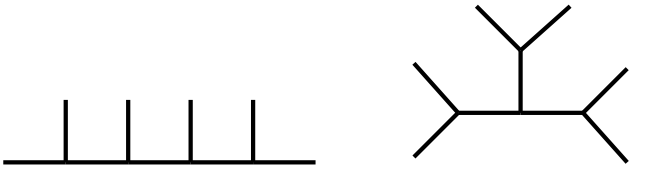

(a) Half-ladder graph. *(b) Branched graph.*

Figure 3: 6 point trees

other.

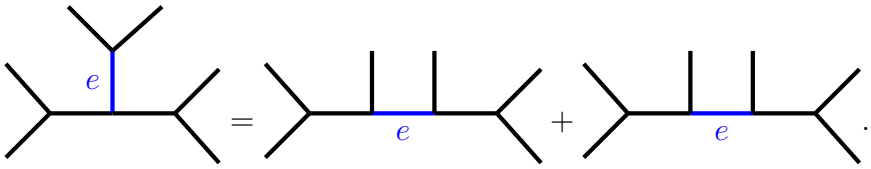

(33)

The full set of Jacobi relations can be found graphically and build a system of equations for the numerators as functions of their diagrammatic representations. The system of equations can be solved for a set of independent kinematic numerator factors. In the end each numerator can be expressed a linear combination of master numerators.

3.2 Examples

The methodology for solving the topology equations is the same regardless of the number of loops or particles. In this section we will go through explicitly the four point case for tree-level and one loop.

3.2.1 Tree level

This is the simplest possible case. For four point tree level we only get one topology. The legs can be ordered in different ways as in Figure 2. Applying the operators $\hat{t}$ and $\hat{u}$ to the diagram with momentum assignment 1234 we get the following equation:

$$n_1(k_1, k_3, k_2, k_4) + n_1(k_1, k_4, k_3, k_2) - n_1(k_1, k_2, k_3, k_4) = 0 \tag{34}$$

Or as graphs:

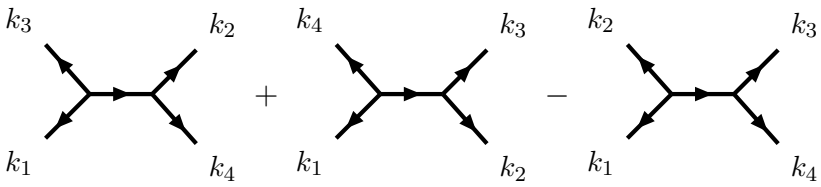

(35)

These are, in principle, the same graphs as in figure fig. 2, but drawn differently to show how the topology of the s-, t-, and u-channel graphs are fundamentally the same. Thus there exists only one topology for the four-point case at tree-level.

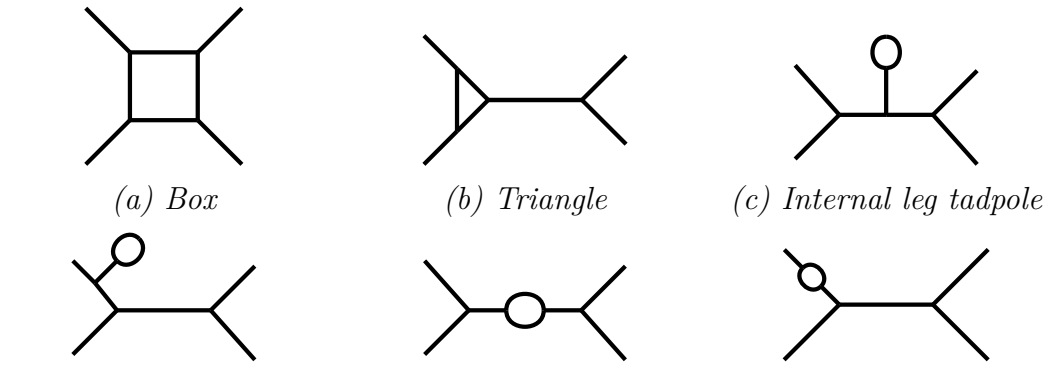

(a) Box *(b) Triangle* *(c) Internal leg tadpole*

(d) External leg tadpole *(e) Internal leg bubble* *(f) External leg bubble*

Figure 4: The six one-loop topologies at four-point level.

3.2.2 One-loop

At one-loop level there are essentially four different types of loops: tadpoles, bubbles, and different types of n-gons. For the four-point one-loop case the n-gons are boxes and triangles. The bubbles and tadpoles can be attached to either an internal or an external leg. For the four-point case this results in a total of six distinct topologies shown in fig. 4.

Applying the $\hat{t}$- and $\hat{u}$- operator to these diagrams we obtain a total of 24 Jacobi equations. Ignoring equations consisting of only one diagram and counting distinct equations only once we end up with a system of equations for the numerator factors as functions of their associated diagrams

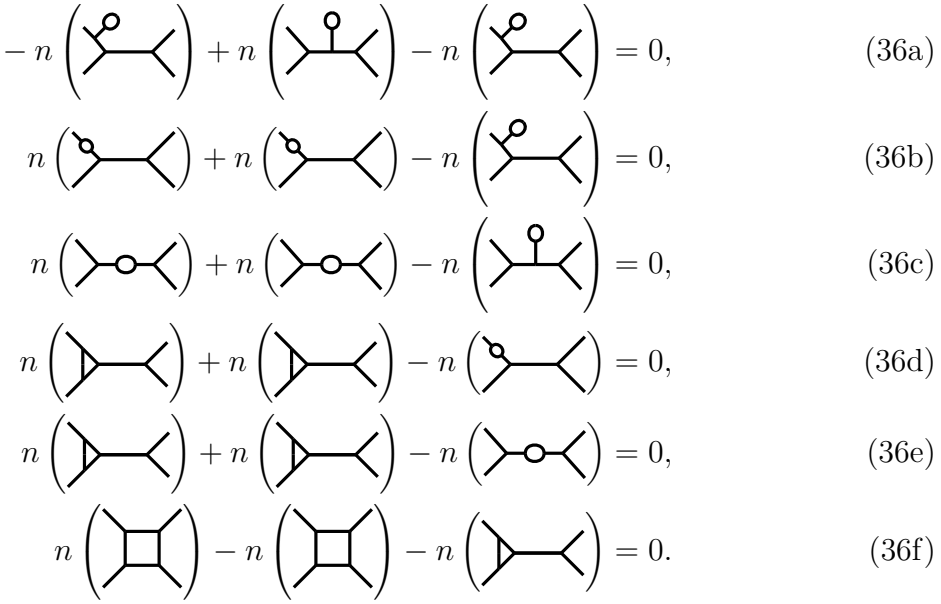

(36a)

(36b)

(36c)

(36d)

(36e)

(36f)

Earlier we stated that graphs are defined by their topology and momentum assignment, yet in solving these equations we care only about the topology for simplicity. It is true that when performing calculations of amplitudes the momentum is important and we would need to include graphs of the same topology but with different momentum assignment to get the full amplitude.

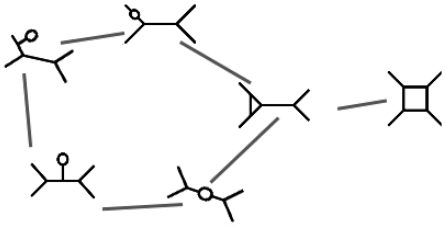

Figure 5: The graph of graphs for the four-point one-loop topologies.

In dropping the momentum assignment we need to keep in mind that two numerators given by the same topology are not necessarily equal. For example we cannot assume that the two box diagram numerators in eq. (36f) cancel each other.

This system of equations can be solved for the box numerator. Meaning all other diagrams can be expressed as linear functions of the box diagram. Starting with eq. (36a) we can isolate the internal bubble diagram and describe it terms of the external leg tadpole diagram, the external leg tadpole diagram we can describe using the external leg bubble, and so on till the box diagram is used to describe every other diagram.

The box diagram however cannot be isolated as in the only equation it appears in it appears twice. Thus it has to be one of the master topologies for this case. As all other diagrams can be described through it it is in fact a unique solution.

How the topologies are related can be shown in a graph of graphs in which every node represents a graph and every edge a relation between the numerators of the graphs. The graph of graphs for the one-loop four-point diagrams is shown in fig. 5. This offers a clear representation of how all numerators apart from the one corresponding to the box diagram are related and how it is possible to transverse the edges between them and cycle around them. The box diagram however has only one edge connecting it to the rest.

3.2.3 Two-loop

At two-loop level for four-point we end up with 48 distinct topologies and a set of 350 equations. There are three topologies through which we can describe all others. It is possible to reduce this to two masters as the three are related through Jacobi equations of the form

n 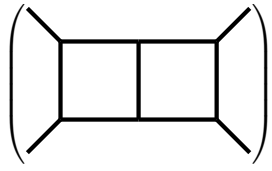 $\pm\, n$ 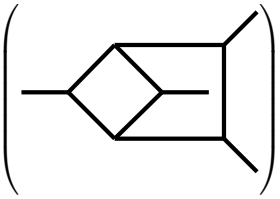 $\pm$ 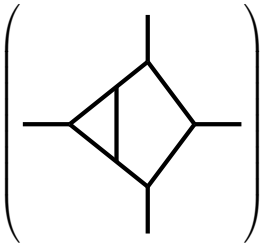 $= 0$ (37)

There are no other equations where either of these numerators can be isolated. One of them can be expressed through the other two but there is no way to reduce the set more than so. Therefore we have a choice in picking the master topologies.

First we want to pick the planar diagram (first in crefeq:4oop2) because of its symmetric properties. One other motivation for picking a master is that it should make the expressions for the other numerators as short as possible. From the two diagrams left we find that the planar diagram with the triangle (last in crefeq:4oop2) appears more often in the equations than the non-planar diagram (middle of crefeq:4oop2). We find that three other diagrams can be expressed directly through the triangle diagram while only one other diagram can be described directly through the non-planar diagram. The number of diagrams that can be constructed directly from the planar diagram is two so from this viewpoint it is a good choice too.

Following this reasoning the final masters are chosen to be the two planar diagrams.

4 RESULTS

In this section we present the main results of the thesis by first describing the code that was written to generate diagrams and equations to solve. We then present the master topologies found at tree-level, one-loop, and two-loop.

4.1 Generating equations

To generate the sets of equations the algorithm was implemented in MATLAB [14]. The code consists of a number of functions that together can generate diagrams and perform operations on them.

MATLABs digraph objects are used to represent the diagrams. These are graphs with directed edges between the nodes and they can be described by two vectors, one containing the source nodes and one containing the target nodes. We let the direction of the edge represent the flow of momenta and as therefore all external nodes are target nodes.

The digraph class allows for attributes to be assigned to the nodes and edges of a graph. In the code used we assign two such attributes to the nodes. The first attribute is `type` which described if the node is external or internal. The second is `name` which is simply a labelling convention to easily distinguish internal nodes from external ones. Knowing which nodes are external and internal we are able to know which edges are external or internal too and can assign similar attributes to the edges. Using attributes like these is useful as we need to keep track of the nodes and edges when performing operations on the graphs.

Two functions are written to generate diagrams, one for which the input was the number of external legs and the output all the tree-level diagrams with that number of external legs. The other works by inputting diagrams and increasing their loop-order by adding one of each of the different loop types to every diagram in the set that was the input. These functions generate diagrams with all possible momentum assignment which is of importance when calculating amplitudes or simply for studying the full set of graphs. However as we only study topologies different versions of the functions were written that only output one diagram of each topology. Cell arrays, which are arrays where any data type can be stored in the cells, are used to store the graphs.

We write two functions `uoperator` and `toperator` to work as the operators $\hat{u}$ and $\hat{t}$. The input for these functions is a digraph object and an edge to operate on. The functions

then switches the edges connected to the nodes of the edge as described in section 3.1 and outputs a new digraph object.

The function to generate the set of equations uses a cell array of topologically distinct diagrams as input and the output is a cell array with the rows representing the Jacobi equations. It works by going through the entire input array and finding the equations for each diagram. This is done by calling the functions `uoperator` and `toperator` for every internal edge in the graph and outputting one new digraph object each. There exists a graph isomorphism between two graphs if the only thing differing between their structure is the ordering of their nodes. We check the isomorphism between the new diagrams and those in the input array to determine the topology of the new diagrams.

In the output for the function to generate equations each cell element is itself a cell array with the first element being the index of the topology and the remaining the momenta. So if there is a graph with topology equal to that of the first graph in the input array and momentum assignment k_1, k_2, k_3, k_4 the corresponding array would be {`1 k1 k2 k3 k3`}. The order of these arrays in the row is that the first element corresponds to the output graph from the `toperator` function, the second the output graph from the `uoperator` function, and the last the original graph.

Thus when all edges of all graphs have been run through we get a set of equations that we can proceed to solve manually.

4.2 Tree level master

For tree-level the system of equations was generated up to the eight-point case. As seen for both the four-point and five-point case there is one topology and for the six-point case there are two. The same is true for the seven-point case as there is an odd number of external edges and we need two to meet at a vertex at each end which leaves only two different ways to position the remaining three edges. For the eight point case there are four distinct topologies.

There is a total of twenty equations for the eight-point case that can be reduced to three since many are identical. Expressed diagrammatically these are

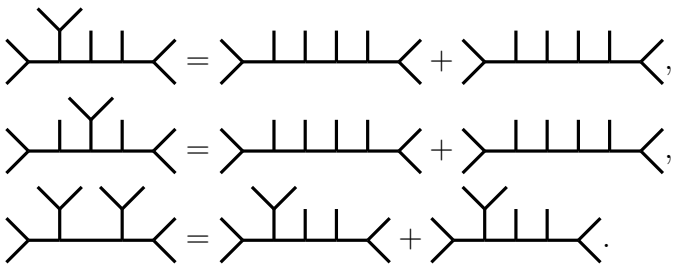

(38a)

(38b)

(38c)

Both diagrams on the left hand side in eqs. (38a) and (38b) are a linear combination of half-ladder diagrams. The third diagram in eq. (38c) is not directly expressed through the half-ladder but as it is a combination of diagrams of the same type as that in eq. (38a) and can therefore be expressed through the half-ladder too. Furthermore none of the equations allow us to isolate the half-ladder graph on either side and solve for it. Regardless of the number of external legs it will always be a function of itself together with another graph.

What we find is that there is that the half-ladder graph is a solution for tree-level numerators regardless of the number of external legs. Even more the solution is unique and there is no possible solution excluding the half-ladder. Consider a half-ladder with $2{+}n+m$ external legs, as on the left hand side in eq. (39). Applying the operators $\hat{t}$ and $\hat{u}$ on the labelled (blue) edge yields the diagrams on the right hand side

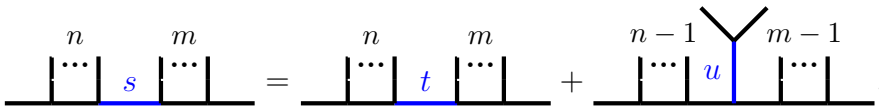

(39)

There are two important observations to make from this set of equations. First that half-ladder graphs can be turned into branched graphs, it is trivial that if we continue the process of applying these operators on the branched graph to the right it will keep branching. Thus from the half-ladder any branched graph can be generated.

More importantly is that in the Jacobi relation for the kinematic numerators of the half-ladder diagram it will always appear twice and thus cannot be isolated. Therefore we conclude that this is a unique solution at tree-level regardless of the number of legs.

4.3 One-loop master

In section 3.2.2 we find that the unique one-loop master topology at four-point is the box diagram. As for the tree-level this is a result easily generalised to hold for any number of external legs.

The relation we find for the box diagram at four-point is that it is directly related to the triangle diagram. Similarly for the five-point case there is a direct relation between the pentagon and the box diagram as the Jacobi relations in eqs. (40a) and (40b) show,

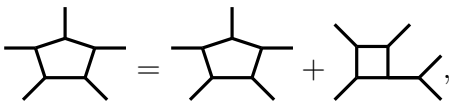

(40a)

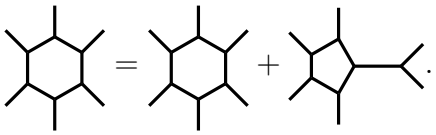

(40b)

This type of relation exist in the set of equations for every one-loop diagrams with n external legs. The equations for the n-gons always include another n-gon and one $(n-1)$-gon. For a diagram with $n{+}m$ external legs the Jacobi equation we get is

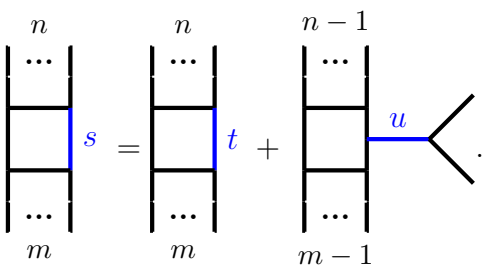

(41)

As in the four-point case it is possible to construct any other one-loop diagram by applying the operators on an edge in the n-gon and then repeating this procedure on the $(n-1)$-gon and so on until all topologies are constructed. Furthermore, as for tree-level half-ladder, the n-gon is a unique solution as it appears twice in eq. (41) and thus cannot be represented in terms of other diagrams.

4.4 Two-loop masters

At the two-loop case equations were generated up to six-point and similar results to that of the four-point case in section 3.2.3. For both the five- and six-point a set of planar and non-planar graphs built up of n-gons (i.e. no branching like the triangle graph at four-point) that could only be expressed through each other. This holds for any number of legs as it follows from the result at one-loop in section 4.3 that any other type of loop can be transformed into a n-gon. Here we are simply following the same procedure for multiple loops at a time.

For both cases this set can be solved for the planar diagrams, a total of two at five-point and three at six-point. That non-planar diagrams always can be related to planar diagrams is shown in fig. 6. An operator, for example $\hat{t}$ as in the figure, is applied to an internal edge and the external edge previously "inside" is brought "outside". This can be repeated for any number of edges.

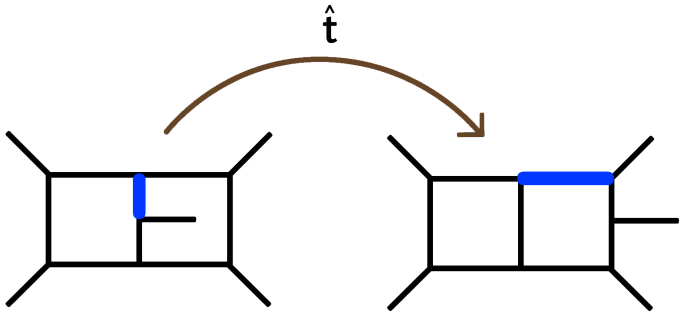

Figure 6: How a non-planar graph can be turned into a planar one by applying an operator on the bold, blue edge.

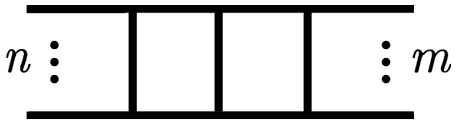

Figure 7: The type of topology for the diagrams that construct the two-loop set of masters.

Thus we can solve for diagrams with topology as depicted in fig. 7. The integers n and m in the figure are always are greater than 0 and when added together sums up to the

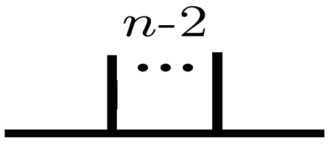

(a) Tree-level master.

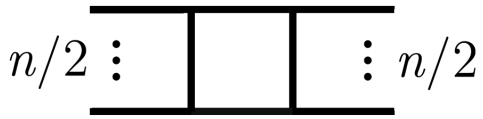

(b) One-loop master.

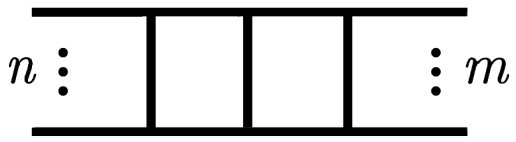

(c) Two-loop master.

Figure 8: The master topologies for the tree-level, one-loop, and two-loop cases.

total number of external legs. This can be described mathematically

$$\begin{aligned} n &= (1, \ldots, \left\lfloor \frac{N}{2} \right\rfloor), \\ m &= N - n, \end{aligned} \tag{42}$$

where N is the total number of external legs. The number of master topologies thus equal $\left\lfloor \frac{N}{2} \right\rfloor$.

For any number of legs this set cannot be reduced further. When applying the operators to the internal edges of the planar diagrams there is a limited amount of outcomes, none of which are two different planar diagrams. The planar diagrams always appear in the Jacobi relations together with another planar diagram and one non-planar.

4.5 Summary of results

We will here summarize the results found previously in this section for clarity.

1. For the tree-level case there is one unique solution that is the numerator associated with the half-ladder topology, see fig. 8a.
2. For the one-loop level there is also one unique solution that is the n-gon,fig. 8b.
3. For the two-loop case there is a set of masters and as such no unique solution. One set that can always be chosen consists of all planar diagrams as in fig. 8c. The number of masters in this set is equal to $\left\lfloor \frac{N}{2} \right\rfloor$, with N being the number of external legs.

5 CONCLUSION AND OUTLOOK

We have reviewed methods for calculating scattering amplitudes by starting with color decomposition and working our way forward. By imposing the color-kinematics duality we showed that many of the partial amplitudes contributing to the full amplitude can be related through Jacobi identities thus reducing the number of needed amplitudes vastly.

The double copy between gravity and gauge theories demonstrates how the field of scattering amplitudes can be used to discover previously unknown relations between theories. That the complicated expressions for gravity amplitudes can be reduced to expression similar to those of gauge theory implies that the dynamics of gravity theories may be a lot less complicated than they appear to be.

In section 3.1 we showed how the numerators for color-ordered diagrams can be reduced to a set associated with a set of independent numerators and associated topologies. Such topologies were found for the tree-level, one-loop, and two-loop cases and generalised for any number of external legs. As an example of the effectiveness of such a reduction the total number of distinct topologies for the six-point two-loop is 674 while the total number of masters is three. Thus the numerators for all color-ordered diagrams can be described using the numerators associated with three topologies.

One evident way to continue this work would be to extend it to more loops as we have only found masters up to two-loops. The same procedure should be applied to more loop levels to find master topologies for these. It would be very useful if a pattern could be discovered between the masters for higher loops such that a generalisation for any number of loops can be made.

Another way to continue would be to look at amplitudes involving more types of particles as we have only concerned ourselves with different types of bosons. It would be interesting to study if, and if so how, the topologies associated with the master numerators change when matter particles are included.

It is needless to say that the field of research amplitudes is filled with opportunities and (hopefully) even more symmetries and relations to be discovered.

ACKNOWLEDGEMENTS

First and foremost I would like to thank my supervisor Gregor Kälin for introducing and guiding me through such a fascinating topic that I would not mind returning to in the future. I would also like to thank all my friends and my parents (plus our dog), for their support and being there for me when my MATLAB code would not work.

REFERENCES

[1] M. E. Peskin and D. V. Schroeder. *An Introduction to Quantum Field Theory*. Addison-Wesley, 1995.

[2] Z. Bern, J. J. M. Carrasco, and H. Johansson. New Relations for Gauge-Theory Amplitudes. *Phys. Rev.*, D78:085011, 2008.

[3] Theodor Schuster. Color ordering in QCD. *Phys. Rev.*, D89(10):105022, 2014.

[4] Lance J. Dixon. Calculating scattering amplitudes efficiently. In *QCD and beyond. Proceedings, Theoretical Advanced Study Institute in Elementary Particle Physics, TASI-95, Boulder, USA, June 4-30, 1995*, pages 539–584, 1996.

[5] Henrik Johansson and Alexander Ochirov. Color-Kinematics Duality for QCD Amplitudes. *JHEP*, 01:170, 2016.

[6] Zvi Bern, John Joseph M. Carrasco, and Henrik Johansson. Perturbative Quantum Gravity as a Double Copy of Gauge Theory. *Phys. Rev. Lett.*, 105:061602, 2010.

[7] Ronald Kleiss and Hans Kuijf. Multi - Gluon Cross-sections and Five Jet Production at Hadron Colliders. *Nucl. Phys.*, B312:616–644, 1989.

[8] Vittorio Del Duca, Lance J. Dixon, and Fabio Maltoni. New color decompositions for gauge amplitudes at tree and loop level. *Nucl. Phys.*, B571:51–70, 2000.

[9] Bo Feng, Rijun Huang, and Yin Jia. Gauge Amplitude Identities by On-shell Recursion Relation in S-matrix Program. *Phys. Lett.*, B695:350–353, 2011.

[10] Yi-Xin Chen, Yi-Jian Du, and Bo Feng. A Proof of the Explicit Minimal-basis Expansion of Tree Amplitudes in Gauge Field Theory. *JHEP*, 02:112, 2011.

[11] Freddy Cachazo. Fundamental BCJ Relation in N=4 SYM From The Connected Formulation. 2012.

[12] N. E. J. Bjerrum-Bohr, Poul H. Damgaard, and Pierre Vanhove. Minimal Basis for Gauge Theory Amplitudes. *Phys. Rev. Lett.*, 103:161602, 2009.

[13] Henriette Elvang and Yu-tin Huang. Scattering Amplitudes. 2013.

[14] MATLAB. *version 9.3.0 (R2017b)*. The MathWorks Inc., Natick, Massachusetts, 2017.

[15] Joshua Ellis. TikZ-Feynman: Feynman diagrams with TikZ. *Comput. Phys. Commun.*, 210:103–123, 2017.